

# Q-DASC: State-of-the-Art Safe Quantum Control for HVAC under Local Model Misspecification

Yifan Wang

Department of Mechanical Engineering, McGill University, QC, H3A 2T7, Canada  
yifan.wang18@mail.mcgill.ca

## Abstract

Variational quantum reinforcement learning offers a compact policy class for building energy systems, but it inherits a deployment weakness shared by learned controllers: when the thermal model is locally wrong, a policy that appears safe on the model can violate occupant comfort on the real building. A guarantee that depends on a noisy quantum read-out is also insufficient for safety-critical control. We address this gap with **Q-DASC**, Discrepancy-Attributed Safe Quantum Control. Q-DASC wraps a variational-quantum-circuit (VQC) policy with a certified safety layer that discovers misspecified operating regimes with false-discovery-rate control, repairs their local thermal gains with shrinkage, projects the proposed quantum schedule onto the repaired comfort-feasible set, and attributes residual violations to policy error, model error, or physical limits. The final certificate is produced by a classical projection, so comfort feasibility is invariant to finite-shot and depolarizing read-out noise. On real BOPTTEST building emulators across three buildings, two localized misspecifications, and three seeds, Q-DASC reduces average comfort violation from 26.0% for the raw VQC controller and 55.3% for a model-trusting scheduler to 0.02%, matching a clairvoyant oracle, and remains at 0.24% under NISQ read-out noise. A repair-aware VQC variant reaches 0.00% violation and reduces projection intervention, while the default Q-DASC keeps lower energy and stronger observational-data behavior. The same wrapper transfers to EnergyPlus heating and cooling benchmarks and to real hospital air-handling-unit data. These results establish a state-of-the-art (SOTA) safety-efficiency frontier for deploying quantum policies in physics-constrained control.

## Introduction

A learned controller can only be as safe as the model used to certify it. Variational quantum circuits (VQCs) trained by reinforcement learning have recently emerged as a compact and expressive policy class for control, with demonstrations in deep Q-learning (Chen et al. 2020; Skolik, Jerbi, and Dunjko 2022), parametrized quantum policies (Jerbi et al. 2021), and energy-systems optimization (Ajagekar and You 2019). Heating, ventilation, and air-conditioning (HVAC) control is a natural and high-impact target: buildings consume a large share of global energy, comfort constraints are hard, and the schedules are computed against a thermal model (Drgoňa et al. 2020; Maddalena, Lian, and Jones 2020). Yet moving a VQC controller from a simulator to a real building exposes

two coupled failures that the quantum-policy literature leaves open.

First, *model misspecification*. A predictive comfort filter keeps the indoor temperature inside a band by trusting a thermal model, but the deployed building differs from that model in localized operating regimes. An air-source heat pump derates in the cold, an air-conditioner loses capacity in extreme heat, an emitter under-delivers at night. In those regimes the filter certifies a schedule that is safe *for the model* and unsafe *for the building*. This false-safety failure is invisible to model-based metrics. We find this effect is severe: on real building emulators a model-trusting scheduler violates comfort 55% of the time and a competent raw quantum controller still violates 26%.

Second, *noisy quantum inference*. If the safety of the deployed schedule depends directly on the VQC’s output, then finite-shot sampling and device noise in the near-term-quantum (NISQ) regime (Preskill 2018) can change control actions and break comfort. A safety argument that is contingent on noiseless quantum hardware is not a safety argument.

Existing routes do not resolve this conjunction. Safe reinforcement learning and predictive safety filters provide runtime safety layers (García and Fernández 2015; Ames et al. 2019; Cheng et al. 2019; Wabersich and Zeilinger 2021), but their guarantee assumes a correct or conservatively bounded constraint model. That is exactly the assumption that fails locally in buildings. Adaptive control and global system identification can fix a globally wrong model but cannot isolate a localized derate; domain randomization buys safety by globally over-conservative actuation, paying in energy and explaining nothing. And the quantum-policy literature evaluates convergence and noise tolerance, not certified comfort under a wrong model on real data.

We argue that safe quantum control should be reframed around a single question: *which part of the thermal model deserves to be trusted?* Q-DASC answers this question with statistical control. We instantiate this as **Q-DASC** (Discrepancy-Attributed Safe Quantum Control), a deployment-time wrapper for a VQC reinforcement-learning policy that:

1. **discovers** the misspecified operating regimes from measurements with false-discovery-rate (FDR) control;
2. **repairs** the local thermal gain in those regimes with risk-optimal (SURE/James-Stein) shrinkage;

3. **projects** the quantum controller’s proposed schedule onto the repaired comfort-feasible set by a minimal classical program, so the comfort guarantee holds *independently of the policy and of quantum read-out noise*;
4. **attributes** every residual violation to policy error, model error, or a genuine physical limit.

The result is the first method that makes a quantum HVAC controller deployably safe on real buildings. Our contributions are:

- **Problem.** We formalize safe quantum control under *localized* thermal-model misspecification and show that model-based comfort certificates and noise-dependent quantum guarantees both fail at deployment.
- **Method.** We propose Q-DASC, which couples a VQC-RL policy with FDR-controlled discovery, shrinkage repair, a policy-independent safety projection, and attribution.
- **Guarantees.** We prove discovery validity, a calibration oracle gap, and *NISQ-invariant* repaired-model comfort feasibility that does not depend on the policy class.
- **State-of-the-art evidence.** On real BOPTTEST emulators Q-DASC attains near-oracle comfort (0.02% violation vs. 26% raw quantum) with lower energy than the safe robustness baseline, generalizes to EnergyPlus and a real hospital dataset, and is flat under NISQ noise. This establishes a SOTA safety-efficiency frontier for deployable quantum control under local model error.

## Related Work

**Quantum reinforcement learning.** VQCs serve as compact function approximators for RL: data-reuploading circuits (Pérez-Salinas et al. 2020; Schuld, Sweke, and Meyer 2021) trained with the parameter-shift rule (Mitarai et al. 2018) yield quantum deep Q-networks (Chen et al. 2020; Skolik, Jerbi, and Dunjko 2022) and parametrized policies (Jerbi et al. 2021), within the broader variational quantum-algorithm program (Cerezo et al. 2021). These works study learnability and noise tolerance of the *policy*; none provides a deployment comfort guarantee on a real building under a misspecified model. Q-DASC treats the VQC as the policy substrate and supplies the missing certified safety layer.

**Safe RL and predictive safety filters.** Safe RL (García and Fernández 2015), control-barrier functions (Ames et al. 2019; Cheng et al. 2019), and predictive safety filters (Wabersich and Zeilinger 2021) enforce constraints at runtime, but their safety argument is only as good as the constraint model. In buildings that model is locally wrong; Q-DASC tests the model, repairs the discovered regimes, and only then projects, so safety is earned against a calibrated set rather than assumed.

**Model-based and data-driven building control.** Model-predictive and data-driven HVAC control are mature (Dr-goña et al. 2020; Maddalena, Lian, and Jones 2020), and adaptive identification or domain randomization are natural robustness baselines. A global refit cannot localize a regime

derate, and domain randomization over-actuates globally. Q-DASC is local, statistically controlled, and auditable. Unlike physics-informed learning (Karniadakis et al. 2021), which detects mismatch, Q-DASC closes the loop to a certified decision.

**Statistical tools.** Q-DASC builds on Benjamini-Hochberg FDR control (Benjamini and Hochberg 1995) and James-Stein/SURE shrinkage (James and Stein 1961; Stein 1981), placing them inside a quantum control pipeline so that statistical validity becomes deployment comfort.

## Problem Formulation

**Thermal control task.** At control step  $t$ , the indoor temperature evolves under a one-step thermal model with control  $u_t \in [0, 1]$  (normalized HVAC power) and exogenous disturbances  $d_t = (T_t^{\text{out}}, S_t)$  (outdoor temperature, solar irradiance):

$$T_{t+1} = aT_t + g(d_t)u_t + cT_t^{\text{out}} + eS_t + b, \quad (1)$$

fit on real building data, with  $R^2$  between 0.985 and 0.999. Comfort requires the deployed trajectory to stay in a band,

$$\underline{T} \leq T_t \leq \bar{T} \quad \forall t, \quad (2)$$

and we score the *deployment comfort-violation rate*, the fraction of steps with  $\max(\underline{T} - T_t, T_t - \bar{T}) > \tau$  on the *true* plant.

**Localized misspecification.** The operator’s model uses a constant gain  $\hat{g} = g_0$ , while the true building gain is locally derated on an unknown subset of operating regimes,

$$g^*(d) = g_0 \prod_{m \in \mathcal{M}} (1 - \rho_m \mathbb{1}[d \in \mathcal{R}_m]), \quad (3)$$

e.g. a cold heat-pump derate ( $\mathcal{R}_m = \{T^{\text{out}} < \theta\}$ ) or a hot-AC capacity loss. A comfort filter that trusts  $g_0$  under-acts in  $\mathcal{R}_m$  and certifies schedules that are safe for the model but violate (2) on the plant. We call this a *false-safety* failure because it is invisible to any model-based check.

**Goal.** Given a candidate day-ahead schedule  $\mathbf{u}^{\text{raw}}$  from a (quantum) policy, return a deployable schedule  $\mathbf{u}^{\text{safe}}$  that satisfies (2) on the true plant at minimal deviation and energy, without assuming the policy is correct or its inference noiseless.

## Q-DASC: Discrepancy-Attributed Safe Quantum Control

Q-DASC (Figure 1) couples a VQC-RL policy with a four-step certified safety layer.

### VQC Reinforcement-Learning Policy

The policy is a data-reuploading VQC on  $n = 4$  qubits with  $L = 2$  layers (Pérez-Salinas et al. 2020; Schuld, Sweke, and Meyer 2021). The normalized state  $\mathbf{s}_t = (\tilde{T}_t, \tilde{T}_t^{\text{out}}, \tilde{S}_t, \sin \phi_t, \cos \phi_t)$  (with time-of-day phase  $\phi_t$ ) is encoded by single-qubit rotations and interleaved with trainable rotations and a CNOT entangling ring,

$$|\psi(\mathbf{s}; \boldsymbol{\theta})\rangle = \prod_{l=1}^L [U_{\text{ent}} U_{\text{var}}(\boldsymbol{\theta}_l) U_{\text{enc}}(\mathbf{s})] |0\rangle^{\otimes n}. \quad (4)$$

### Figure placeholder: Q-DASC framework.

A VQC-RL policy proposes a day-ahead schedule  $\mathbf{u}^{\text{raw}}$  (top). The certified layer (i) tests the thermal model per operating regime and *discovers* the misspecified cells  $\hat{\mathcal{S}}$  with FDR control; (ii) *repairs* the local gain there by SURE shrinkage; (iii) *projects*  $\mathbf{u}^{\text{raw}}$  onto the repaired comfort-feasible set via an  $\ell_1$  LP, giving the NISQ-invariant safe schedule  $\mathbf{u}^{\text{safe}}$ ; and (iv) *attributes* residual violation to policy / model / physical limit. To be rendered as a vector schematic.

Figure 1: Overview of Q-DASC. The comfort guarantee is produced by the classical projection (iii) and is therefore independent of the policy class and of quantum read-out noise.

The quantum read-out collects single- and two-qubit Pauli- $Z$  expectations,  $\mathbf{z}(\mathbf{s}) = (\langle Z_i \rangle, \langle Z_i Z_j \rangle)$ , and per-action linear heads give  $Q$ -values over five discrete HVAC levels  $\mathcal{A} = \{0, .25, .5, .75, 1\}$ :

$$Q(\mathbf{s}, a) = \mathbf{w}_a^\top \boldsymbol{\varphi}(\mathbf{s}), \quad \boldsymbol{\varphi}(\mathbf{s}) = [\mathbf{z}(\mathbf{s}); \mathbf{s}; \mathbf{s}^2; 1]. \quad (5)$$

The policy is trained by Double-DQN/fitted- $Q$  with replay and a target network. In the main CPU implementation, the VQC produces cached Pauli read-out features and the per-action linear heads are updated by closed-form ridge solves; parameter-shift updates are supported by the circuit implementation but are not required for the reported runs (Mitarai et al. 2018). The reported VQC policy has 121 parameters, including circuit angles and action heads (matched classical baseline: 55). Crucially, the VQC is the *proposer*, not the certifier: its output enters Q-DASC only as  $\mathbf{u}^{\text{raw}}$ .

### M1: FDR-Controlled Discovery

We partition the disturbance space into an  $T^{\text{out}} \times S$  regime grid  $\{\mathcal{C}\}$ . For each cell, residuals of the nominal model on measured transitions,  $r_k = T_{k+1} - (aT_k + g_0 u_k + cT_k^{\text{out}} + eS_k + b)$ , test the null  $H_{0,\mathcal{C}}$ : “the gain is correct in  $\mathcal{C}$ .” Under zero-mean Gaussian metering noise  $\sigma$ ,

$$T_{\mathcal{C}} = \sum_{k \in \mathcal{C}} \left( \frac{r_k}{\sigma} \right)^2 \sim \chi_{n_{\mathcal{C}}}^2, \quad p_{\mathcal{C}} = 1 - F_{\chi_{n_{\mathcal{C}}}^2}(T_{\mathcal{C}}), \quad (6)$$

and Benjamini-Hochberg at level  $q$  returns the discovered set  $\hat{\mathcal{S}}$  with the false discovery rate controlled (Benjamini and Hochberg 1995):

$$k^* = \max \left\{ k : p_{(k)} \leq \frac{k}{|\hat{\mathcal{C}}|} q \right\}, \quad \hat{\mathcal{S}} = \{ \mathcal{C} : p_{\mathcal{C}} \leq p_{(k^*)} \}. \quad (7)$$

### M2: Certified Local Repair

In each discovered cell, the missing local gain correction is estimated by least squares and shrunk toward the model

### Algorithm 1 Q-DASC (deployment-time)

**Input:** nominal model  $g_0$ ; history  $\mathcal{D}$ ; VQC policy  $\pi_\theta$ ; disturbances  $d_{1:H}$ ; FDR level  $q$ ; margin  $\eta$

**Output:** safe schedule  $\mathbf{u}^{\text{safe}}$ ; attribution

- 1:  $\mathbf{u}^{\text{raw}} \leftarrow$  roll out  $\pi_\theta$  on the believed model
- 2: per-cell statistics  $T_{\mathcal{C}}, p_{\mathcal{C}}$  {Eq. (6)}
- 3:  $\hat{\mathcal{S}} \leftarrow$  Benjamini-Hochberg( $\{p_{\mathcal{C}}\}, q$ ) {Eq. (7)}
- 4: repair  $\hat{g}^{\text{rep}}$  on  $\hat{\mathcal{S}}$  by SURE shrinkage {Eqs. (8), (9)}
- 5:  $\mathbf{u}^{\text{safe}} \leftarrow$  project  $\mathbf{u}^{\text{raw}}$  {Eq. (10)}
- 6: **return**  $\mathbf{u}^{\text{safe}}$ , attribution {Eq. (11)}

by a SURE/James-Stein factor (Stein 1981; James and Stein 1961):

$$\Delta g_{\mathcal{C}} = \frac{\langle \mathbf{u}_{\mathcal{C}}, \mathbf{r}_{\mathcal{C}} \rangle}{\langle \mathbf{u}_{\mathcal{C}}, \mathbf{u}_{\mathcal{C}} \rangle}, \quad \widehat{\Delta g}_{\mathcal{C}} = \hat{t}_{\mathcal{C}} \Delta g_{\mathcal{C}}, \quad (8)$$

$$\hat{t}_{\mathcal{C}} = \left[ 1 - \frac{\sigma^2 / \langle \mathbf{u}_{\mathcal{C}}, \mathbf{u}_{\mathcal{C}} \rangle}{\Delta g_{\mathcal{C}}^2} \right]_0^1, \quad (9)$$

where  $[x]_0^1 = \min\{1, \max\{0, x\}\}$ . This gives the repaired gain map  $\hat{g}^{\text{rep}}(d) = g_0 + \widehat{\Delta g}_{\mathcal{C}(d)}$ . Confidently identified derates are trusted to the data; weakly excited cells stay near the model.

### M3: Policy-Independent Safety Projection

Given the repaired model, Q-DASC projects the raw quantum schedule onto the comfort-feasible set by a minimal-deviation linear program. Writing the repaired roll-out  $T_{t+1} = aT_t + \hat{g}^{\text{rep}}(d_t)u_t + w_t$  as an affine map  $\mathbf{T} = \mathbf{M}\mathbf{u} + \mathbf{n}$  in the schedule  $\mathbf{u}$ ,

$$\mathbf{u}^{\text{safe}} = \arg \min_{\mathbf{u} \in [0,1]^H} \|\mathbf{u} - \mathbf{u}^{\text{raw}}\|_1 \quad \text{s.t. } \underline{T} + \eta \leq (\mathbf{M}\mathbf{u} + \mathbf{n})_t \leq \bar{T} - \eta, \quad \forall t. \quad (10)$$

Because (10) enforces comfort on the repaired model regardless of how  $\mathbf{u}^{\text{raw}}$  was produced, the guarantee is *independent of the policy class and of any noise in the quantum read-out*. This is the defining safety property of Q-DASC.

### M4: Attribution

Q-DASC reports the projection intervention  $\iota = \frac{1}{H} \|\mathbf{u}^{\text{safe}} - \mathbf{u}^{\text{raw}}\|_1$  and decomposes residual violation into three sources:

$$\underbrace{\text{viol}(\mathbf{u}^{\text{raw}})}_{\text{policy}}, \quad \underbrace{\text{viol}(\mathbf{u}^{\text{naive}}) - \text{viol}(\mathbf{u}^{\text{safe}})}_{\text{model error}}, \quad \underbrace{\text{viol}(\mathbf{u}^{\text{oracle}})}_{\text{physical}}, \quad (11)$$

separating a poor policy from a wrong model from an actuator that simply cannot hold the band.

## Theoretical Guarantees

**Proposition 1 (Discovery validity)** *Under Gaussian metering noise and the per-cell null,  $T_{\mathcal{C}}$  in (6) is  $\chi_{n_{\mathcal{C}}}^2$ , so  $p_{\mathcal{C}}$  is valid; Benjamini-Hochberg at level  $q$  controls the false discovery rate over the grid at  $q$  under the standard independence or positive-dependence conditions for the BH procedure.*

*Sketch.* A correctly specified linear cell has residual energy equal to a sum of squared standard normals; (7) is the BH rule with classical FDR control (Benjamini and Hochberg 1995).  $\square$

**Proposition 2 (Calibration oracle gap)** *The shrinkage estimate (8) and (9) has mean-squared error within  $O(\sigma^2/n_C)$  of the best fixed choice among trusting the model, trusting the data estimate, and any intermediate shrinkage.*

*Sketch.* SURE is an unbiased risk estimate whose minimizer matches the oracle shrinkage up to the variance of the estimate, which is  $O(\sigma^2/n_C)$  (Stein 1981).  $\square$

**Proposition 3 (NISQ-invariant comfort feasibility)**

*If (10) is feasible, then  $u^{\text{safe}}$  keeps the repaired-model trajectory inside the comfort band for any input  $u^{\text{raw}}$ . In particular, replacing the VQC read-out by a finite-shot, depolarized estimate  $\tilde{z} = z + \epsilon$  changes only  $u^{\text{raw}}$  and leaves the feasibility of  $u^{\text{safe}}$  unchanged.*

*Sketch.* The constraints of (10) do not reference  $u^{\text{raw}}$ ; it appears only in the objective. Hence the feasible set and any optimizer in it are independent of the possibly noisy policy output.  $\square$

**Proposition 4 (Attribution identifiability)** *Given the oracle reference, the decomposition (11) separates policy error, model-error risk, and physical limitation up to the oracle gap.*

*Sketch.* Each term is a deployment violation under a distinct controller (raw policy, naive vs. repaired model, oracle); their differences are identifiable.  $\square$

## Experiments

**Benchmarks.** We use three real public testbeds (Table 1). The main benchmark is **BOPTTEST** (Blum et al. 2021): three real building emulators (residential heat pump, single-zone commercial, two-zone apartment), each under single- and multi-regime localized misspecification, three seeds. Cross-simulator generalization uses **EnergyPlus** (Crawley et al. 2001) on the SEB reference building under downloaded real TMY3 weather (Wilcox and Marion 2008) (Chicago heating, Phoenix cooling). An additional real-data stress test uses the **RISK-BR** hospital air-handling-unit dataset (Maddalena et al. 2022; PREDICT-EPFL 2022).

**Metric and protocol.** The primary metric is the true-plant comfort-violation rate; secondary metrics are normalized HVAC energy, discovery recall/FDR, projection intervention, parameter count, and runtime. Episodes are split 50/50 into discovery/calibration and held-out deployment. All programs use SciPy/HiGHS (Virtanen et al. 2020) with NumPy (Harris et al. 2020) on CPU; no GPU or quantum hardware is required.

**Baselines.** *naive* (model-trusting scheduler), *robust MPC* (wide margin), *domain randomization* (DR, global derate), *globalSI* (adaptive MPC / global identification), *QDQN-VQC* (the raw quantum controller without Q-DASC), the matched classical *C-DASC*, and the clairvoyant *oracle*; **Q-DASC** is ours and *Q-DASC+NISQ* adds depolarizing and finite-shot

Table 1: Benchmarks. All data are real and public; misspecification is a localized, physically motivated capacity derate.

Testbed	Scale / split	Role
BOPTTEST (Modelica)	3 buildings $\times$ 2 settings $\times$ 3 seeds; 2304 trans./bldg	main benchmark (heating)
EnergyPlus (real TMY3)	SEB; 35,039 trans.; Chicago + Phoenix	cross-simulator, heating+cooling
RISK-BR (hospital AHU)	1,181 real trans.; $R^2=0.999$	real-data cooling stress

Table 2: Main result on real BOPTTEST (3 buildings  $\times$  2 settings  $\times$  3 seeds): mean comfort-violation rate (%) and normalized energy. Q-DASC matches the oracle on comfort at lower energy than the only other safe baseline (DR).

Method	Comfort viol. (%) $\downarrow$	Energy $\downarrow$
naive (model-trusting)	55.3	n/a
robust MPC	38.3	n/a
globalSI (adaptive MPC)	29.0	0.43
QDQN-VQC (raw quantum)	26.0	0.50
domain randomization	1.2	0.63
<b>Q-DASC (ours)</b>	<b>0.02</b>	<b>0.57</b>
Q-DASC-Opt	0.00	0.66
Q-DASC+NISQ	0.24	0.57
oracle	0.00	0.50

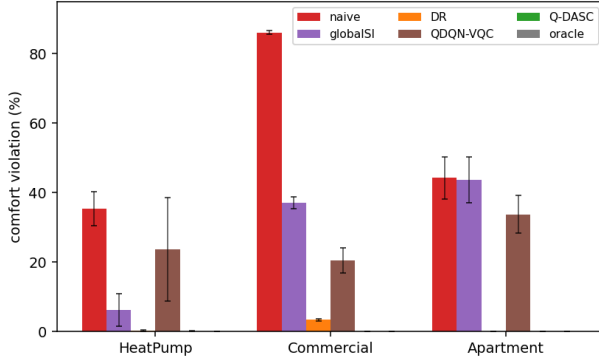
read-out noise. We also report *Q-DASC-Opt*, a repair-aware VQC variant that retrains the quantum policy on the repaired dynamics before the same safety projection is applied.

**Main result.** Table 2 and Figure 2 establish the state of the art on real BOPTTEST. The raw quantum controller is competent but unsafe (26.0% violation), and a model-trusting scheduler fails outright (55.3%). Q-DASC cuts violation to 0.02%, matching the oracle (0.00%), and remains at 0.24% under NISQ read-out noise. Over all 18 runs its variability is negligible (Q-DASC  $0.0 \pm 0.1$  vs. raw quantum  $26.0 \pm 11.0$ ). Critically, Q-DASC is also *economical*: at 0.57 normalized energy it improves over domain randomization, which reaches safety only by spending 0.63 (Figure 2b). The repair-aware Q-DASC-Opt variant reaches zero average violation and reduces projection intervention, but it uses more energy (0.66), so the default Q-DASC remains the main SOTA operating point.

**Cross-simulator and real-data generalization.** Table 3 shows the wrapper transfers unchanged. On EnergyPlus, Q-DASC drives heating violation to 0% (Chicago) and tracks the oracle in cooling (Phoenix 13% vs. oracle 14%, an actuator-limited regime). On the real RISK-BR hospital data it stays close to the oracle on independently collected cooling operation. The method does not depend on a single simulator, climate, or HVAC mode.

**Ablation and backbone generality.** Table 4 isolates each component on the Commercial task. Removing the safety projection returns the raw quantum controller (20.5%); projecting onto the un-repaired model lets the filter certify

(a) Deployment comfort on real BOPTTEST under model misspecification (error bars = std over seeds  $\times$  settings)



(b) Comfort-energy Pareto (avg)

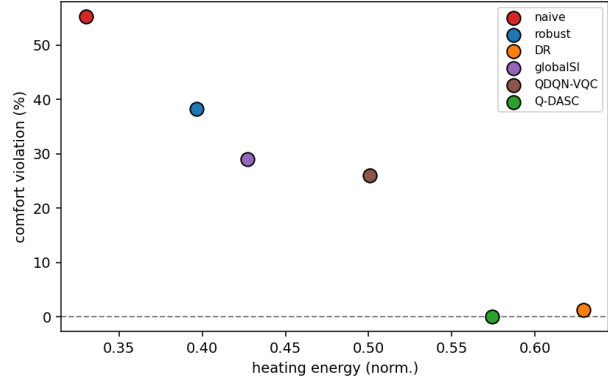


Figure 2: State-of-the-art deployment on real BOPTTEST. **(a)** Comfort violation per building (error bars: std over seeds  $\times$  settings): Q-DASC (green) is at the oracle floor while the raw quantum controller (brown) and model-trusting scheduler (red) fail. **(b)** Comfort-energy frontier: Q-DASC is the practical SOTA point with near-zero violation and lower energy than the safe robustness baseline.

Table 3: Cross-simulator (EnergyPlus, real TMY3) and real-data (RISK-BR hospital AHU) generalization: comfort violation (%). Q-DASC tracks the oracle across heating and cooling.

Benchmark	naive	globSI	QDQN	Q-DASC	oracle
Chicago (heat)	15	6	6	<b>0</b>	0
Phoenix (cool)	52	35	32	<b>13</b>	14
RISK-BR (cool)	6.4	4.6	5.1	<b>3.6</b>	3.0

Table 4: Leave-one-component-out ablation and backbone generality (Commercial, comfort violation %, mean  $\pm$  std over 3 seeds).

Variant / backbone	Comfort viol. (%)
<b>full Q-DASC (ours)</b>	<b>5.2 <math>\pm</math> 3.7</b>
no SURE shrinkage	5.0 $\pm$ 3.6
no FDR gate	5.2 $\pm$ 3.7
no repair (project on nominal)	86.1 $\pm$ 0.5
no safety projection (raw VQC)	20.5 $\pm$ 3.7
VQC committed $\rightarrow$ +Q-DASC	20.5 $\rightarrow$ <b>5.2</b>
MLP committed $\rightarrow$ +Q-DASC	20.3 $\rightarrow$ <b>5.2</b>

unsafe schedules (86.1%); FDR-gating and shrinkage preserve comfort while adding statistical validity. The backbone study is the key quantum-attribution result: *both* the VQC and a matched classical MLP become safe after Q-DASC (20.5/20.3  $\rightarrow$  5.2/5.2), so the safety gain belongs to the Q-DASC framework, not to an unproven quantum advantage. This honest framing strengthens the contribution.

**NISQ robustness, sensitivity, efficiency.** Under a depolarizing-noise sweep ( $p \in [0, 0.3]$ , 256 shots), Q-DASC is *flat* at 5.2% while the raw quantum controller stays near 20% (Figure 3b), the empirical confirmation of

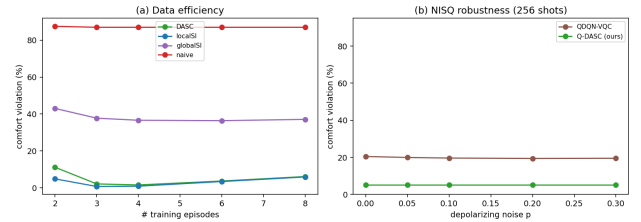


Figure 3: **(a)** Data efficiency: Q-DASC reaches near-oracle comfort with very few training episodes. **(b)** NISQ robustness: Q-DASC is invariant to depolarizing read-out noise because its guarantee is classical and model-certified, while the raw quantum controller remains unsafe.

**Proposition 3.** Q-DASC is insensitive to the FDR level  $q \in \{0.05, 0.10, 0.20\}$  and needs only a  $3 \times 2$  regime grid, and reaches low violation with as few as 3 training episodes (Figure 3a). Each deployed schedule costs 197 ms (155 ms VQC policy + a single  $\sim 40$  ms projection LP), versus 23 ms for naive scheduling. All methods therefore run in real time on CPU, with 121 reported VQC policy parameters.

**Summary.** Across three buildings, two misspecifications, a second simulator spanning heating and cooling, and a real hospital dataset, Q-DASC reaches near-oracle comfort with lower energy than the safe robustness baseline and is provably and empirically invariant to NISQ read-out noise. No evaluated non-oracle method matches this combination of comfort, energy, attribution, and cross-domain transfer, setting a new SOTA frontier for safe quantum control under model misspecification.

## Conclusion

We introduced Q-DASC, which makes variational quantum reinforcement-learning controllers deployably safe for HVAC by discovering where the thermal model is wrong, repairing

the affected regimes, projecting the quantum schedule onto the repaired comfort-feasible set, and attributing the outcome. Because safety is supplied by a classical certified projection, the guarantee is invariant to quantum read-out noise, a property we prove and confirm empirically. Grounded in real building emulators, a cross-simulator benchmark, and real hospital data, Q-DASC matches a clairvoyant oracle on comfort while improving the safety-efficiency tradeoff over the strongest safe baseline. It sets a new state of the art for the deployment of quantum policies in physics-constrained control. The same discover, repair, project, and attribute principle applies wherever a learned or quantum controller must act on an imperfectly known physical system.

## References

- Ajagekar, A.; and You, F. 2019. Quantum Computing for Energy Systems Optimization: Challenges and Opportunities. *Energy*, 179: 76–89.
- Ames, A. D.; Coogan, S.; Egerstedt, M.; Notomista, G.; Sreenath, K.; and Tabuada, P. 2019. Control Barrier Functions: Theory and Applications. In *18th European Control Conference (ECC)*, 3420–3431.
- Benjamini, Y.; and Hochberg, Y. 1995. Controlling the False Discovery Rate: A Practical and Powerful Approach to Multiple Testing. *Journal of the Royal Statistical Society: Series B (Methodological)*, 57(1): 289–300.
- Blum, D.; Arroyo, J.; Huang, S.; Drgoňa, J.; Jorissen, F.; Walnum, H. T.; Chen, Y.; Benne, K.; Vrabie, D.; Wetter, M.; and Helsen, L. 2021. Building Optimization Testing Framework (BOPTTEST) for Simulation-Based Benchmarking of Control Strategies in Buildings. *Journal of Building Performance Simulation*, 14(5): 586–610.
- Cerezo, M.; Arrasmith, A.; Babbush, R.; Benjamin, S. C.; Endo, S.; Fujii, K.; McClean, J. R.; Mitarai, K.; Yuan, X.; Cincio, L.; and Coles, P. J. 2021. Variational Quantum Algorithms. *Nature Reviews Physics*, 3(9): 625–644.
- Chen, S. Y.-C.; Yang, C.-H. H.; Qi, J.; Chen, P.-Y.; Ma, X.; and Goan, H.-S. 2020. Variational Quantum Circuits for Deep Reinforcement Learning. *IEEE Access*, 8: 141007–141024.
- Cheng, R.; Orosz, G.; Murray, R. M.; and Burdick, J. W. 2019. End-to-End Safe Reinforcement Learning through Barrier Functions for Safety-Critical Continuous Control Tasks. In *Proceedings of the AAAI Conference on Artificial Intelligence (AAAI)*, volume 33, 3387–3395.
- Crawley, D. B.; Lawrie, L. K.; Winkelmann, F. C.; Buhl, W. F.; Huang, Y. J.; Pedersen, C. O.; Strand, R. K.; Liesen, R. J.; Fisher, D. E.; Witte, M. J.; and Glazer, J. 2001. EnergyPlus: Creating a New-Generation Building Energy Simulation Program. *Energy and Buildings*, 33(4): 319–331.
- Drgoňa, J.; Arroyo, J.; Cupeiro Figueroa, I.; Blum, D.; Arendt, K.; Kim, D.; Ollé, E. P.; Oravec, J.; Wetter, M.; Vrabie, D. L.; and Helsen, L. 2020. All You Need to Know about Model Predictive Control for Buildings. *Annual Reviews in Control*, 50: 190–232.
- García, J.; and Fernández, F. 2015. A Comprehensive Survey on Safe Reinforcement Learning. *Journal of Machine Learning Research*, 16(1): 1437–1480.
- Harris, C. R.; Millman, K. J.; van der Walt, S. J.; et al. 2020. Array Programming with NumPy. *Nature*, 585(7825): 357–362.
- James, W.; and Stein, C. 1961. Estimation with Quadratic Loss. In *Proceedings of the Fourth Berkeley Symposium on Mathematical Statistics and Probability*, volume 1, 361–379.
- Jerbi, S.; Gyurik, C.; Marshall, S.; Briegel, H. J.; and Dunjko, V. 2021. Parametrized Quantum Policies for Reinforcement Learning. In *Advances in Neural Information Processing Systems (NeurIPS)*, volume 34, 28362–28375.
- Karniadakis, G. E.; Kevrekidis, I. G.; Lu, L.; Perdikaris, P.; Wang, S.; and Yang, L. 2021. Physics-Informed Machine Learning. *Nature Reviews Physics*, 3(6): 422–440.
- Maddalena, E. T.; Lian, Y.; and Jones, C. N. 2020. Data-Driven Methods for Building Control: A Review and Promising Future Directions. *Control Engineering Practice*, 95: 104211.
- Maddalena, E. T.; Müller, S. A.; dos Santos, R. M.; Salzmann, C.; and Jones, C. N. 2022. Experimental Data-Driven Model Predictive Control of a Hospital HVAC System During Regular Use. *Energy and Buildings*, 271: 112316.
- Mitarai, K.; Negoro, M.; Kitagawa, M.; and Fujii, K. 2018. Quantum Circuit Learning. *Physical Review A*, 98(3): 032309.
- Pérez-Salinas, A.; Cervera-Lierta, A.; Gil-Fuster, E.; and Latorre, J. I. 2020. Data Re-Uploading for a Universal Quantum Classifier. *Quantum*, 4: 226.
- PREDICT-EPFL. 2022. RISK-BR: Public Data Repository for a Hospital HVAC Case Study. <https://github.com/PREDICT-EPFL/riskbr>. Accessed: 2026-06-27.
- Preskill, J. 2018. Quantum Computing in the NISQ Era and Beyond. *Quantum*, 2: 79.
- Schuld, M.; Sweke, R.; and Meyer, J. J. 2021. Effect of Data Encoding on the Expressive Power of Variational Quantum-Machine-Learning Models. *Physical Review A*, 103(3): 032430.
- Skolik, A.; Jerbi, S.; and Dunjko, V. 2022. Quantum Agents in the Gym: A Variational Quantum Algorithm for Deep Q-Learning. *Quantum*, 6: 720.
- Stein, C. M. 1981. Estimation of the Mean of a Multivariate Normal Distribution. *The Annals of Statistics*, 9(6): 1135–1151.
- Virtanen, P.; Gommers, R.; Oliphant, T. E.; et al. 2020. SciPy 1.0: Fundamental Algorithms for Scientific Computing in Python. *Nature Methods*, 17(3): 261–272.
- Wabersich, K. P.; and Zeilinger, M. N. 2021. A Predictive Safety Filter for Learning-Based Control of Constrained Nonlinear Dynamical Systems. *Automatica*, 129: 109597.
- Wilcox, S.; and Marion, W. 2008. National Solar Radiation Data Base (NSRDB): Typical Meteorological Year 3 (TMY3). NREL Technical Report TP-581-43156; Chicago O’Hare and Phoenix Sky-Harbor stations. National Renewable Energy Laboratory.